

# Purely two-dimensional vortex matter in infinite-layer nickelates

D. Sanchez-Manzano<sup>1</sup>, V. Humbert<sup>1</sup>, A. Gutiérrez-Llorente<sup>2,1</sup>, D. Zhang<sup>1</sup>, J. Santamaría<sup>3</sup>, M. Bibes<sup>1</sup>, L. Iglesias<sup>1,\*</sup>, Javier E. Villegas<sup>1,&</sup>

<sup>1</sup>*Laboratoire Albert Fert, CNRS, Thales, Université Paris-Saclay, 91767 Palaiseau, France*

<sup>2</sup>*Escuela Superior de Ciencias Experimentales y Tecnología, Universidad Rey Juan Carlos, 28933 Madrid, Spain*

<sup>3</sup>*GFMC, Dpto. de Física de Materiales, Facultad de Ciencias Físicas, Universidad Complutense de Madrid, 28040 Madrid, Spain*

\* [lucia.iglesias@cnrs-thales.fr](mailto:lucia.iglesias@cnrs-thales.fr)

& [javier.villegas@cnrs-thales.fr](mailto:javier.villegas@cnrs-thales.fr)

**Characterizing the dimensionality of the superconducting state in the infinite-layer (IL) nickelates is crucial to understand its nature. Most studies have addressed the problem by studying the anisotropy of the upper critical fields. Yet, the dominance of Pauli-paramagnetism effects over orbital ones makes it challenging to interpret the experiments in terms of dimensionality. Here we address the question from a different perspective, by investigating the vortex phase diagram in the mixed-state. We demonstrate that superconducting  $\text{Pr}_{0.8}\text{Sr}_{0.2}\text{NiO}_2$  thin films present a vortex liquid-to-glass transition of a purely two-dimensional nature. The obtained results suggest that bidimensionality is an intrinsic property, and that superconductivity resides in fully-decoupled  $\text{NiO}_2$  planes. In this scenario, the coherence length along the c-axis must be shorter than the distance between those planes, while Josephson and magnetostatic coupling between them must be negligible. We believe that these conclusions are relevant for theories on the origin of superconductivity in the IL-nickelates.**

Since the discovery of superconductivity in infinite layer (IL) nickelates [1], many efforts have focused on finding analogies and differences with the cuprates, [2,3] with which they share electron counts ( $\text{Ni}^{1+}:\text{3d}^9$ ) and a square planar geometry in the basal plane. The underlying idea is that both families of materials could also share pairing mechanisms –which is still under debate [4]– and that such a quest may help solve the longstanding problem of high-temperature superconductivity. Work has been devoted e.g., to searching d-wave superconductivity [5], charge density waves [6–9], and the strange metal behavior above  $T_c$  [10] that characterizes the cuprates. The research has also unveiled differences with the latter materials. For example, unlike the cuprates’ parent compound, which is a robust antiferromagnetic insulator, undoped IL nickelates show bad-metal behavior and the possible existence of long-range antiferromagnetism is still under debate [6,11–13].

Superconductivity in IL-nickelates has been observed only in ultrathin films. On the other hand, these materials present a layered, intrinsically anisotropic structure with  $\text{NiO}_2$  planes separated by a rare-earth/hole dopant (Nd, Pr, La, Sr, Ca) [1]. Those characteristics have motivated much recent work to elucidate the anisotropy and dimensionality of the superconducting phase. This has been done by measuring the upper critical field  $H_{c2}$  along different crystallographic directions [14–20]. A variety of behaviors have been observed, interpreted in some cases in terms of highly anisotropic [17–19] and in others isotropic [14–16] superconductivity, with a strong dependence on the rare-earth element [18] and doping level [15]. The main problem, as detailed below, is that the competition between orbital-limited and Pauli-limited superconductivity –depending on the field direction and temperature [14]– makes it difficult to interpret that phenomenology in terms of dimensionality.

Despite being a key to characterizing the superconducting state, vortex physics in the IL-nickelates has so far received relatively scarce attention [21,22], and little is known about the vortex phase diagram and dynamics. In the cuprates’ mixed-state, the interplay between thermal

effects, anisotropy, vortex elasticity, and structural disorder results in a complicated vortex-phase diagram, thoroughly studied [23]. Clean single-crystals show a zero-resistance vortex-solid phase at low temperatures, separated by a first-order “melting” transition from dissipative vortex-liquid [24]. In thin films, due to disorder, that transition becomes a continuous second-order one at a temperature  $T_g$  that separates the vortex liquid from a vortex glass. Contrary to the solid, the glass presents no long-range translational order [23,25]. Whether this phenomenology is present in IL-nickelate films remains unexplored. One of the reasons why that question is of great interest is, precisely, because the glass transition is extremely sensitive to the dimensionality of the superconducting state. This is so because the vortex-glass correlation length  $\xi_{VG}$  must diverge upon approaching the glass phase from the liquid one; however, that is hindered in systems of reduced dimensionality. In particular, in truly two-dimensional systems,  $\xi_{VG}$  can only diverge along two spatial directions, resulting in  $T_g = 0$  [26]. This has dramatic effects on the electrical transport properties: it implies that, strictly speaking, a truly zero-resistance state is only achieved at 0 K.

Here we study vortex dynamics in the mixed state of infinite-layer  $\text{Pr}_{0.8}\text{Sr}_{0.2}\text{NiO}_2$  (IL-PSNO) thin films and find clear evidence of purely two-dimensional vortex matter. We find that the two-dimensional character of superconductivity is intrinsic. This suggests that superconductivity resides within the  $\text{NiO}_2$  planes and there exists virtually no coupling between them.

Optimally doped perovskite  $\text{Pr}_{0.8}\text{Sr}_{0.2}\text{NiO}_3$  (PV-PSNO) thin films were epitaxially grown on (001)  $\text{SrTiO}_3$  (STO) by pulsed laser deposition (PLD). A capping layer of  $\sim 2$  nm STO was deposited on the nickelate film to help stabilize the infinite-layer structure [6,27]. Following the same procedure described in previous work [28], the as-grown samples underwent a subsequent  $\text{CaH}_2$  reduction process to obtain the  $\text{Pr}_{0.8}\text{Sr}_{0.2}\text{NiO}_2$  (IL-PSNO) infinite-layer phase. Figure 1 (a) displays the X-ray diffraction data ( $\theta$ - $2\theta$  scan around  $c$  axis, Cu  $K\text{-}\alpha$  radiation) for

the sample before (red) and after (black) reduction, showing a shift of the (002) peak from 48.4° (PV-PSNO) to 54.8° as expected for a complete transformation into the infinite layer phase (IL-PSNO). Low-angle X-Ray reflectivity (not shown) allowed us to measure the film thickness  $d = 7.9 \text{ nm} \pm 0.2 \text{ nm}$ .

In Fig. 1 (b)-(c), the zero-field resistance *vs.* temperature  $R(T)$  shows a superconducting transition with critical temperature  $T_C \sim 7.2 \text{ K}$  as defined by the criterion  $R = 0.5R_N$  ( $R_N = 178 \Omega$  is the normal-state resistance at  $T = 10 \text{ K}$ ). Under the application of magnetic fields (see legend) the superconducting transition widens, as expected. This effect is much stronger when  $H$  is applied along the crystallographic  $c$  axis [perpendicular to the film, Fig. 1(c)] than when it is applied parallel to the  $ab$  plane [parallel to the film, Fig. 1(b)]. This anisotropic behavior is comparable to that observed in  $\text{La}_{0.8}\text{Sr}_{0.2}\text{NiO}_2$  [15,17,20] (IL-LSNO) films, and stronger than in  $\text{Nd}_{0.775}\text{Sr}_{0.225}\text{NiO}_2$  ones (IL-NSNO) [14,20]. Resistance *vs.* magnetic field measurements with  $H$  applied along the  $c$  axis [Fig. 1 (d)] and in-plane (see Supplemental Material) display typical superconducting behavior, qualitatively as expected nickelate films [14]. Based on those measurements and using the criterion  $R = 0.5R_N$ , we calculated the temperature-dependent upper critical fields  $H_{C2}$ , which are displayed in Fig. 1 (e).  $H_{c2,\perp}$  (along  $c$ , black symbols) shows a linear behavior while the  $H_{c2,\parallel}$  (parallel to the  $ab$  plane, red symbols) shows a square root dependence, as expected in the Ginzburg-Landau (GL) approximation for films whose thickness  $d$  limits the divergence of the coherence length [29], that is:

$$(1) \quad H_{c2,\perp}(T) = \frac{\phi_0}{2\pi\xi_{ab}^2(0)} (1 - T/T_C)$$

$$(2) \quad H_{c2,\parallel}(T) = \frac{\sqrt{12}\phi_0}{2\pi d\xi_{ab}(0)} (1 - T/T_C)^{0.5}$$

From  $H_{c2,\perp}(T)$  in Fig. 1 (e) and using Eq. 1, we calculate the temperature-dependent GL coherence length in the  $ab$  plane (see inset) and its zero-temperature value  $\xi_{ab}(0) \sim 3.7 \text{ nm}$ .

This value is comparable to  $\xi_{ab}(0)$  for  $\text{Nd}_{0.775}\text{Sr}_{0.225}\text{NiO}_2$  (IL-NSNO) films [1,14,30,31]. Just as in [14], we find a quantitative inconsistency for  $H_{C2,\parallel}(T)$ : its value is between 32% and 68% of that expected from Eq. 2 with  $d = 7.9$  nm. This suggests that  $H_{C2,\parallel}$  is Pauli-limited [14,32], i.e., that it is determined by paramagnetic (Zeeman energy) effects and not by orbital ones. In this scenario,  $H_{C2,\parallel}$  is unrelated to  $d$  and the coherence length ( $\xi_{ab}, \xi_c$ ), and it is instead given by  $H_{C2,\parallel} = H_p = \Delta_0(T)/\sqrt{2}\mu$ , with  $\Delta_0(T) = \Delta_0(0)(1 - T/T_C)^{0.5}$  the zero-field temperature-dependent superconducting energy gap and  $\mu$  the effective in-plane electronic magnetic moment. Based on the data in Fig. 1 (b), and assuming BCS behavior  $\Delta_0(0) = 1.76k_B T_C$ , we obtain  $\mu \sim 0.5\mu_B$ . This is similar to values reported elsewhere for IL-PSNO [20] and IL-LSNO [15,17] and suggests a depressed magnetic susceptibility as compared to the free-electron system ( $\mu = \mu_B$ ) that contrasts with the enhanced  $\mu \sim 2.4\mu_B$  obtained under the same assumptions for IL-NSNO [14]. The possible origin of this diverse phenomenology, currently debated, includes rare-earth's magnetism effects [20] and unconventional (triplet) superconducting pairing [15].

In summary, we observe a strongly anisotropic behavior in the critical fields, however, the temperature dependence in parallel configuration follows the behavior expected for Pauli-limited superconductivity with an anomalous  $\mu \sim 0.5\mu_B$ . This implies that the ratio  $\gamma = H_{C2,\parallel}/H_{C2,\perp}$  does not reflect the anisotropy in the superconducting coherence length  $\xi_{ab}/\xi_c$ , which could be much higher than  $\gamma$ . It also suggests that studies on the angular-dependent critical fields and magnetoresistance in the nickelates [18] may be difficult to interpret in terms of the vortex matter dimensionality.

Clear evidence of the two-dimensional nature of vortex matter in IL-PSNO is obtained from low-current  $R(T)$  measurements with  $H$  applied perpendicular to the film, which are displayed

in Fig. 2. For all fields,  $\log(R)$  vs.  $1000/T$  is linear across a large portion of the resistive transition, demonstrating activated behavior,

$$(3) R \propto e^{\frac{-U(H)}{k_B T}},$$

as expected in the thermally activated flux-flow regime [23]. The inset of Fig. 2 displays the field-dependent vortex activation energy  $U(H)$  calculated from the linear fits shown in the main panel. Two distinct field regimes are observed. At high fields ( $\mu_0 H > 1$  T), when collective vortex pinning expectedly dominates [23], we observe  $U(H) \propto -\log(H)$ . This is characteristic of two-dimensional vortex matter [23], as observed in a variety of systems including the most anisotropic cuprates [33–35]. Such a field dependence is in stark contrast with  $U(H) \propto H^{-\alpha}$  observed in 3D superconductors, including moderately anisotropic cuprates such as  $\text{YBa}_2\text{Cu}_3\text{O}_7$  for which  $0.5 < \alpha < 1$  [36], and also superconducting IL-NSNO for which an unusual  $\alpha > 5$  has been reported [14]. For low fields ( $\mu_0 H < 1$  T), the field dependence of  $U$  becomes weaker, as observed also for other IL-nickelate films [14], suggesting a crossover into a single-vortex pinning regime [23]. Notice finally that in the  $\log(R)$  vs.  $1000/T$  there exists a systematic departure from activated behavior at low temperatures: the measured resistance exceeds the trend dictated by Eq. 3 (dashed straight line). This occurs below a departure temperature  $T_d$  (and below a resistance level) that is lower (higher) the stronger the magnetic field. Such behavior suggests the onset of a crossover from thermally activated vortex motion into a different regime, possibly the quantum motion of vortices [37] observed in a variety of two-dimensional systems [33,38–40].

Further evidence of purely two-dimensional vortex matter is provided by sets of isothermal  $V(I)$  measured in fixed magnetic fields, as those shown in Fig. 3 (a). The behavior is the same for all the fields studied  $0.1 \text{ T} < \mu_0 H < 5 \text{ T}$ . At the highest temperatures, the response is ohmic within the entire current range. Upon cooling, the ohmic range gradually narrows:  $V(I)$

becomes nonlinear above a certain  $I_{nl}$  that decreases as the temperature is decreased, together with the ohmic resistance  $R_{lin} = \lim_{I \rightarrow 0} V/I$ . This behavior is as expected across a continuous (second-order) transition from a non-superconducting vortex-liquid into a vortex-glass [25,41–47] in which, below a certain transition temperature  $T_g$ , the concavity of the  $V(I)$  should change from upward to downward, yielding a truly superconducting state with  $\lim_{I \rightarrow 0} V/I = 0$ . However, in Fig. 3 (a) all  $V(I)$  are concave up. This indicates either a finite  $T_g$  that lies below the floor temperature of our experiments ( $\sim 1.8$  K), or that the system is purely two-dimensional, in which case  $T_g = 0$  [26,48]. The latter scenario is demonstrated by the collapse of the  $V(I)$  isotherms into a single master curve, achieved via the scaling ansatz from the vortex-glass theory for two-dimensional systems [26,48–50]:

$$(4) \quad \frac{V}{I} \cdot e^{\left(\frac{T_0}{T}\right)^p} = f\left(\frac{I}{T^{1+\nu_{2D}}}\right)$$

where  $f$  is a (field-dependent) universal function for all  $T$ ,  $T_0$  is a characteristic energy scale, the critical exponent  $\nu_{2D} = 2$ , and  $p$  reflects the dominant transport mechanism, with  $p \geq 1$  for thermal activation of vortices and  $p \approx 0.7$  expected for quantum tunneling of vortices across the relevant energy barriers [51]. From the theory, it follows that the ohmic resistance in the low-current limit is:

$$(5) \quad R_{lin} \propto e^{-\left(\frac{T_0}{T}\right)^p}$$

Figure 3 (b) displays the collapse of the  $V(I)$  from Fig. 3 (a) according to Eq. 4. That is achieved by fixing  $p = 1$  (in consistency with Fig. 2, where vortex motion is thermally activated across most of the resistive transition) and finding the value of  $T_0$  that allows collapsing all  $V(I)$  onto a single master curve. The highest  $T$  isotherms, those with  $R_{lin} > 0.5R_N$ , are excluded from this analysis in agreement with the  $H_{c2}$  criterion [see Fig. 1 (d)]. Similarly,  $R_{lin}$  data points for  $T < T_d$  (temperature of deviation from activated behavior, see Fig. 2) cannot be scaled and are

also excluded. Notice however that the non-linear (high-current) data points from the latter isotherms do collapse onto the master curve.

The above approach allows collapsing the set of  $V(I)$  for each of the studied fields, and thus determining  $T_0(H)$ , with a typical error bar  $\Delta T_0 \sim 10\%$  (see Supplemental Material). Notably,  $T_0(H)$  [inset of Fig. 3 (b)] is qualitatively and quantitatively similar to  $U(H)$  shown in the inset of Fig. 2. This evidences the consistency of the analysis –while  $U(H)$  dictates the temperature-dependent transport at a fixed low-current level,  $T_0(H)$  governs the scaling of both temperature and current effects over the entire dynamic range (linear and nonlinear regimes).

In summary, the scaling analysis indicates that vortex matter is purely two-dimensional in IL-PSNO, leading to a vortex-glass transition with  $T_g=0$ . Additional supporting evidence is given in the Supplemental Material, where we illustrate that the scaling of the  $V(I)$  datasets is not possible within the frame of 3D or quasi-2D glass transition models.

Based on the scaling parameter  $T_0$ , we can estimate an upper limit for the vortex length  $l$  along the  $c$ -axis. According to earlier work [49,52],  $T_0$  is of the same order of magnitude as the vortex core energy, that is  $k_B T_0 \approx \varepsilon_0 l$  with the vortex core energy per unit length  $\varepsilon_0 = \hbar \rho_S / m$ . Assuming a Cooper pair mass  $m = 1.82 \cdot 10^{-30}$  kg and density  $\rho_S = 10^{27}$  m<sup>-3</sup> as in the cuprates (IL-PSNO presents a normal carrier density [28,53] similar to the cuprates) and considering that  $T_0 < 40$  K [from Fig. 3(b)], we obtain  $l < 0.1$  nm. This length scale is two orders of magnitude shorter than the film thickness, which indicates that the pure 2D behavior is an intrinsic property and not a thin film geometry effect. Further, the estimated  $l$  is 3 times shorter than the distance between NiO<sub>2</sub> planes in the structure. From this, two possible pictures come to mind.

The first one is that superconductivity in IL-PSNO may be an interfacial effect, analogously as in the LAO/STO and Al/KTO systems [54,55], in which superconductivity emerges from a two-dimensional electron gas. In that scenario, vortices would be naturally two-dimensional as



vortex correlations along the c-axis  $\xi_{VG,\perp}$  are not defined. This picture would also be consistent with Pauli-limited superconductivity in parallel applied fields. However, the experimental evidence rules out a two-dimensional electron gas at the interface between IL nickelates and the SrTiO<sub>3</sub> substrate [56]. Further, IL nickelates have successfully been grown on other substrates, such as LSAT, in which the formation of 2D gases is hindered [57]. Therefore, the interfacial superconductivity scenario seems unlikely, unless some novel state different from a 2D electron gas can be postulated as a precursor of superconductivity.

In the second picture, also fully compatible with Pauli-limited behavior, is that superconductivity resides in the NiO<sub>2</sub> planes, and these are fully decoupled from one another. This suggests that the coherence length in the c-axis is much shorter than the distance between NiO<sub>2</sub> planes, and that Josephson and magnetostatic coupling are negligible [23]. In this scenario, under the application of  $H_{\perp}$ , “pancake vortices” [58] nucleate in each NiO<sub>2</sub> plane that are completely decorrelated from those in the adjacent planes, resulting in  $\xi_{VG,\perp} = 0$ . This situation is analogous to that of the highly anisotropic cuprate TBCCO [52] and strongly oxygen-depleted YBCO [49]. However, there exist two remarkable differences between the case of the cuprates and that of IL-PSNO. The former show a finite  $\xi_{VG,\perp}$  and  $T_g$  (3D behavior) at low  $\mu_0 H_{\perp}$ , and the crossover into pure 2D behavior with  $T_g = 0$  is observed only above magnetic fields of the order of  $\sim 1$  T, when the in-plane interactions between vortices overcome the Josephson coupling between superconducting layers (pair of CuO<sub>2</sub> planes) [59]. In contrast, IL-PSNO shows  $T_g = 0$  from the lowest fields  $\sim 0.1$  T. This is even more surprising considering that NiO<sub>2</sub> planes are only  $\sim 3$  Å apart while, in the highly anisotropic cuprates, the distance between superconducting layers is in the nanometer range. This situation could be explained by two ingredients. The first one is a relatively long penetration length, that we estimate [60]  $\lambda_0 = 1.29 \times 10^{-2} (\rho/T_c)^{1/2} \sim \mu\text{m}$ , in good agreement with earlier work [1]. This has to be compared with  $\lambda_0 \sim 100$  nm in the cuprates. A longer  $\lambda_0$  significantly enhances vortex interactions within

each NiO<sub>2</sub> plane, which would promptly overcome inter-plane vortex interactions in increasing magnetic field [23]. The second ingredient is the possible magnetism of Pr under magnetic fields [25], which would expectedly contribute to quenching superconducting coupling between NiO<sub>2</sub> planes. Extending the present transport experiments to other IL nickelates would be desirable to clarify those contributions.

In summary, we have studied vortices in the mixed state of superconducting IL-PSNO films. The dynamic scaling of the  $V(I)$  characteristics and field dependence of the vortex activation energy consistently demonstrates that vortex matter is purely two-dimensional in this system, even for fields as low as 0.1 T. The quantitative analysis of the scaling parameters indicates that the vortex length along the c-axis is much shorter than the film thickness and the distance between NiO<sub>2</sub> planes, and thus that the two-dimensional nature of vortex matter is intrinsic. The existing evidence suggests that superconductivity resides within NiO<sub>2</sub> planes and coupling between them is virtually inexistent. We believe that this conclusion is an important ingredient to understanding the nature and origin of superconductivity in the infinite layer nickelates.

### **Acknowledgements**

We acknowledge funding from French ANR through grants ANR-22-CE24-0009-01 “SEEDS”, ANR22-CE30-00020-01 “SUPERFAST”, ANR-22-EXSP-0007 PEPR SPIN “SPINMAT”, and the European Union’s EIC pathfinder grant 101130224 “JOSEPHINE” and the COST action “SUPERQUMAP” . A.G.L. acknowledges financial support through a research grant from the Next Generation EU plan 2021, European Union.

## References

- [1] D. Li, K. Lee, B. Y. Wang, M. Osada, S. Crossley, H. R. Lee, Y. Cui, Y. Hikita, and H. Y. Hwang, Superconductivity in an infinite-layer nickelate, *Nature* **572**, 624 (2019).
- [2] A. S. Botana, F. Bernardini, and A. Cano, Nickelate Superconductors: An Ongoing Dialog between Theory and Experiments, *Journal of Experimental and Theoretical Physics* **132**, 618 (2021).
- [3] B. Y. Wang, K. Lee, and B. H. Goodge, Experimental Progress in Superconducting Nickelates, *Annu Rev Condens Matter Phys* **15**, 305 (2024).
- [4] Á. A. Carrasco Álvarez, L. Iglesias, S. Petit, W. Prellier, M. Bibes, and J. Varignon, Charge ordering as the driving mechanism for superconductivity in rare-earth nickel oxides, *Phys Rev Mater* **8**, 064801 (2024).
- [5] X. Wu, D. Di Sante, T. Schwemmer, W. Hanke, H. Y. Hwang, S. Raghu, and R. Thomale, Robust dx<sub>2</sub>-y<sub>2</sub>-wave superconductivity of infinite-layer nickelates, *Phys Rev B* **101**, 060504 (2020).
- [6] G. Krieger et al., Charge and Spin Order Dichotomy in NdNiO<sub>2</sub> Driven by the Capping Layer, *Phys. Rev. Lett.* **129**, 27002 (2022).
- [7] M. Rossi et al., A broken translational symmetry state in an infinite-layer nickelate, *Nat Phys* **18**, 869 (2022).
- [8] C. C. Tam et al., Charge density waves in infinite-layer NdNiO<sub>2</sub> nickelates, *Nature Materials* 2022 21:10 **21**, 1116 (2022).
- [9] A. Raji, G. Krieger, N. Viart, D. Preziosi, J.-P. Rueff, and A. Gloter, Charge Distribution across Capped and Uncapped Infinite-Layer Neodymium Nickelate Thin Films, *Small* **n/a**, 2304872 (n.d.).
- [10] K. Lee et al., Linear-in-temperature resistivity for optimally superconducting (Nd,Sr)NiO<sub>2</sub>, *Nature* 2023 619:7969 **619**, 288 (2023).
- [11] H. Lu et al., Magnetic excitations in infinite-layer nickelates, *Science* (1979) **373**, 213 (2021).
- [12] J. Fowlie et al., Intrinsic magnetism in superconducting infinite-layer nickelates, *Nature Physics* 2022 18:9 **18**, 1043 (2022).
- [13] X. Zhou et al., Antiferromagnetism in Ni-Based Superconductors, *Advanced Materials* **34**, 2106117 (2022).
- [14] B. Y. Wang, D. Li, B. H. Goodge, K. Lee, M. Osada, S. P. Harvey, L. F. Kourkoutis, M. R. Beasley, and H. Y. Hwang, Isotropic Pauli-limited superconductivity in the infinite-layer nickelate Nd<sub>0.775</sub>Sr<sub>0.225</sub>NiO<sub>2</sub>, *Nature Physics* 2021 17:4 **17**, 473 (2021).
- [15] L. E. Chow et al., Pauli-limit violation in lanthanide infinite-layer nickelate superconductors, *ArXiv* **2204.12606**, (2022).
- [16] B. Y. Wang et al., Rare-Earth Control of the Superconducting Upper Critical Field in Infinite-Layer Nickelates, *ArXiv* **2205.15355**, (2022).
- [17] W. Sun et al., Evidence for Anisotropic Superconductivity Beyond Pauli Limit in Infinite-Layer Lanthanum Nickelates, *Advanced Materials* **35**, 2303400 (2023).

- [18] L. E. Chow et al., Dimensionality control and rotational symmetry breaking superconductivity in square-planar layered nickelates, *ArXiv* **2301.07606**, (2023).
- [19] H. Ji et al., Rotational symmetry breaking in superconducting nickelate Nd<sub>0.8</sub>Sr<sub>0.2</sub>NiO<sub>2</sub> films, *Nature Communications* 2023 14:1 **14**, 1 (2023).
- [20] B. Y. Wang et al., Effects of rare-earth magnetism on the superconducting upper critical field in infinite-layer nickelates, *Sci Adv* **9**, (2023).
- [21] N. P. Quirk, D. Li, B. Y. Wang, H. Y. Hwang, and N. P. Ong, The vortex-Nernst effect in a superconducting infinite-layer nickelate, *ArXiv* **2309.03170**, (2023).
- [22] R. A. Shi, B. Y. Wang, Y. Iguchi, M. Osada, K. Lee, B. H. Goodge, L. F. Kourkoutis, H. Y. Hwang, and K. A. Moler, Scanning SQUID study of ferromagnetism and superconductivity in infinite-layer nickelates, *Phys Rev Mater* **8**, 024802 (2024).
- [23] G. Blatter, M. V. Feigel'man, V. B. Geshkenbein, A. I. Larkin, and V. M. Vinokur, Vortices in high-temperature superconductors, *Rev Mod Phys* **66**, 1125 (1994).
- [24] H. Safar, P. Gammel, D. Huse, D. Bishop, J. Rice, and D. Ginsberg, Experimental evidence for a first-order vortex-lattice-melting transition in untwinned, single crystal YBa<sub>2</sub>Cu<sub>3</sub>O<sub>7</sub>, *Phys Rev Lett* **69**, 824 (1992).
- [25] M. P. Fisher, Vortex-glass superconductivity: a possible new phase in bulk high-T<sub>c</sub> oxides, *Phys Rev Lett* **62**, 1415 (1989).
- [26] C. Dekker, P. J. M. Woltgens, R. H. Koch, B. W. Hussey, and A. Gupta, Absence of a Finite-Temperature Vortex-Glass Phase Transition in Two-Dimensional YBa<sub>2</sub>Cu<sub>3</sub>O<sub>7-tt</sub> Films, *Phys Rev Lett* **69**, 2717 (1992).
- [27] G. Krieger, A. Raji, L. Schlur, G. Versini, C. Bouillet, M. Lenertz, J. Robert, A. Gloter, N. Viart, and D. Preziosi, Synthesis of infinite-layer nickelates and influence of the capping-layer on magnetotransport, *J Phys D Appl Phys* **56**, 024003 (2022).
- [28] A. Gutiérrez-Llorente et al., Toward Reliable Synthesis of Superconducting Infinite Layer Nickelate Thin Films by Topochemical Reduction, *Advanced Science* **11**, 2309092 (2024).
- [29] M. Tinkham, *Introduction to superconductivity*, 296 (1975).
- [30] M. Osada, B. Y. Wang, B. H. Goodge, S. P. Harvey, K. Lee, D. Li, L. F. Kourkoutis, and H. Y. Hwang, Nickelate Superconductivity without Rare-Earth Magnetism: (La,Sr)NiO<sub>2</sub>, *Advanced Materials* **33**, 2104083 (2021).
- [31] S. Zeng et al., Superconductivity in infinite-layer nickelate La<sub>1-x</sub>CaxNiO<sub>2</sub> thin films, *Sci Adv* **8**, 9927 (2022).
- [32] A. M. Clogston, Upper Limit for the Critical Field in Hard Superconductors, *Phys Rev Lett* **9**, 266 (1962).
- [33] A. W. Tsien, B. Hunt, Y. D. Kim, Z. J. Yuan, S. Jia, R. J. Cava, J. Hone, P. Kim, C. R. Dean, and A. N. Pasupathy, Nature of the quantum metal in a two-dimensional crystalline superconductor, *Nature Physics* 2015 12:3 **12**, 208 (2015).
- [34] C. Zhang et al., Observation of two-dimensional superconductivity in an ultrathin iron–arsenic superconductor, *2d Mater* **8**, 025024 (2021).

- [35] A. Yu, T. Zhang, D. Fan, P. Yuan, W. Peng, H. Li, C. Lin, G. Mu, X. Zhang, and L. You, Vortex glass phase transition in two-dimensional Bi<sub>2</sub>Sr<sub>2</sub>Ca<sub>2</sub>Cu<sub>3</sub>O sub-microbridge, *Supercond Sci Technol* **36**, 035008 (2023).
- [36] Z. Sefrioui, D. Arias, E. M. González Lez, C. Leó, J. Santamaria, and J. L. Vicent, Vortex liquid entanglement in irradiated YBa<sub>2</sub>Cu<sub>3</sub>O<sub>7</sub> thin films, *Phys Rev B* **63**, (2001).
- [37] M. P. A. Fisher, Quantum phase transitions in disordered two-dimensional superconductors, *Phys Rev Lett* **65**, 923 (1990).
- [38] D. Ephron, A. Yazdani, A. Kapitulnik, and M. R. Beasley, Observation of Quantum dissipation in the vortex state of a highly disordered superconducting thin film, *Phys Rev Lett* **76**, 1529 (1996).
- [39] Y. Qin, C. L. Vicente, and J. Yoon, Magnetically induced metallic phase in superconducting tantalum films, *Phys Rev B Condens Matter Mater Phys* **73**, 1 (2006).
- [40] Y. Saito, Y. Kasahara, J. Ye, Y. Iwasa, and T. Nojima, Metallic ground state in an ion-gated two-dimensional superconductor, *Science* (1979) **350**, 409 (2015).
- [41] D. S. Fisher, M. P. A. Fisher, and D. A. Huse, Thermal fluctuations, quenched disorder, phase transitions, and transport in type-II superconductors, *Phys Rev B* **43**, 130 (1991).
- [42] H.-J. Kim, Y. Liu, Y. S. Oh, S. Khim, I. Kim, G. R. Stewart, and K. H. Kim, Vortex-glass phase transition and superconductivity in an underdoped (Ba, K)Fe<sub>2</sub>As<sub>2</sub> single crystal, *Phys Rev B* **79**, (2009).
- [43] Q. Li, H. J. Wiesmann, M. Suenaga, L. Motowidlow, and P. Haldar, Observation of vortex-glass-to-liquid transition in the high-T<sub>c</sub> superconductor Bi<sub>2</sub>Sr<sub>2</sub>Ca<sub>2</sub>Cu<sub>3</sub>O<sub>10</sub>, *Phys Rev B* **50**, (1994).
- [44] Z. Sefrioui, D. Arias, M. Varela, J. E. Villegas, M. A. López De La Torre, C. Leó, G. D. Loos, and J. Santamarí, Crossover from a three-dimensional to purely two-dimensional vortex-glass transition in deoxygenated YBa<sub>2</sub>Cu<sub>3</sub>O<sub>7</sub> thin films, *Phys Rev B* **60**, (1999).
- [45] R. H. Koch, V. Foglietti, W. J. Gallagher, G. Koren, A. Gupta, and M. P. A. Fisher, Experimental evidence for vortex-glass superconductivity in Y-Ba-Cu-O, *Phys Rev Lett* **63**, 1511 (1989).
- [46] Z. Sefrioui, D. Arias, C. Leon, J. Santamaria, E. M. Gonzalez, J. L. Vicent, and P. Prieto, Zero-magnetic-field dynamic scaling in Bi<sub>2</sub>Sr<sub>2</sub>CaCu<sub>2</sub>O<sub>8</sub> thin films, *Phys Rev B* **70**, (2004).
- [47] J. E. Villegas and J. L. Vicent, Vortex-glass transitions in low-T<sub>c</sub> superconducting Nb thin films and Nb/Cu superlattices, *Phys Rev B* **71**, (2005).
- [48] H.-H. Wen, H. A. Radovan, F.-M. Kamm, P. Ziemann, S. L. Yan, L. Fang, and M. S. Si, 2D Vortex-Glass Transition with T<sub>g</sub> 50 K in Tl<sub>2</sub>Ba<sub>2</sub>CaCu<sub>2</sub>O<sub>8</sub> Thin Films due to High Magnetic Fields, *Phys Rev Lett* **80**, (1998).
- [49] J. S. Z. Sefrioui, D. Arias, M. Varela, J. E. Villegas, M. A. López de la Torre, C. Leon, G.D. Loos, Crossover from a three-dimensional to purely two-dimensional vortex-glass transition in deoxygenated YBa<sub>2</sub>Cu<sub>3</sub>O<sub>7-x</sub> thin films, *Phys. Rev* **108**, 1175 **60**, 423 (1999).
- [50] J. E. Villegas and J. L. Vicent, Vortex-glass transitions in low- T<sub>c</sub> superconducting Nb thin films and NbCu superlattices, *Phys Rev B Condens Matter Mater Phys* **71**, 1 (2005).

- [51] M. P. A. Fisher, T. A. Tokuyasu, and A. P. Young, Vortex variable-range-hopping resistivity in superconducting films, *Phys Rev Lett* **66**, 2931 (1991).
- [52] H.-H. Wen, H. A. Radovan, F.-M. Kamm, P. Ziemann, S. L. Yan, L. Fang, and M. S. Si, 2D Vortex-Glass Transition with  $T_g = 5.0$  K in  $Tl_2Ba_2CaCu_2O_8$  Thin Films due to High Magnetic Fields, *Phys Rev Lett* **80**, (1998).
- [53] M. Osada, B. Y. Wang, K. Lee, D. Li, and H. Y. Hwang, Phase diagram of infinite layer praseodymium nickelate  $Pr_{1-x}Sr_xNiO_2$  thin films, *Phys Rev Mater* **4**, 121801 (2020).
- [54] N. Reyren et al., Superconducting Interfaces Between Insulating Oxides, *Science* (1979) **317**, 1196 (2007).
- [55] S. Mallik, G. C. Ménard, G. Saïz, H. Witt, J. Lesueur, A. Gloter, L. Benfatto, M. Bibes, and N. Bergeal, Superfluid stiffness of a  $KTaO_3$ -based two-dimensional electron gas, *Nature Communications* 2022 13:1 **13**, 1 (2022).
- [56] B. H. Goodge, B. Geisler, K. Lee, M. Osada, B. Y. Wang, D. Li, H. Y. Hwang, R. Pentcheva, and L. F. Kourkoutis, Resolving the polar interface of infinite-layer nickelate thin films, *Nature Materials* 2023 22:4 **22**, 466 (2023).
- [57] K. Lee et al., Linear-in-temperature resistivity for optimally superconducting  $(Nd,Sr)NiO_2$ , *Nature* 2023 619:7969 **619**, 288 (2023).
- [58] J. R. Clem, Two-dimensional vortices in a stack of thin superconducting films: A model for high-temperature superconducting multilayers, *Phys. Rev. B* **43**, 7837 (1991).
- [59] H. H. Wen, P. Ziemann, H. A. Radovan, and S. L. Yan, Field-induced crossover of criticalities of vortex dynamics in  $Tl_2Ba_2CaCu_2O_8$  thin films, *Europhys Lett* **42**, 319 (1998).
- [60] L. P. Gor'kov, Theory of superconducting alloys in a strong magnetic field near the critical temperature, *JETP* **37**, 1407 (1960).

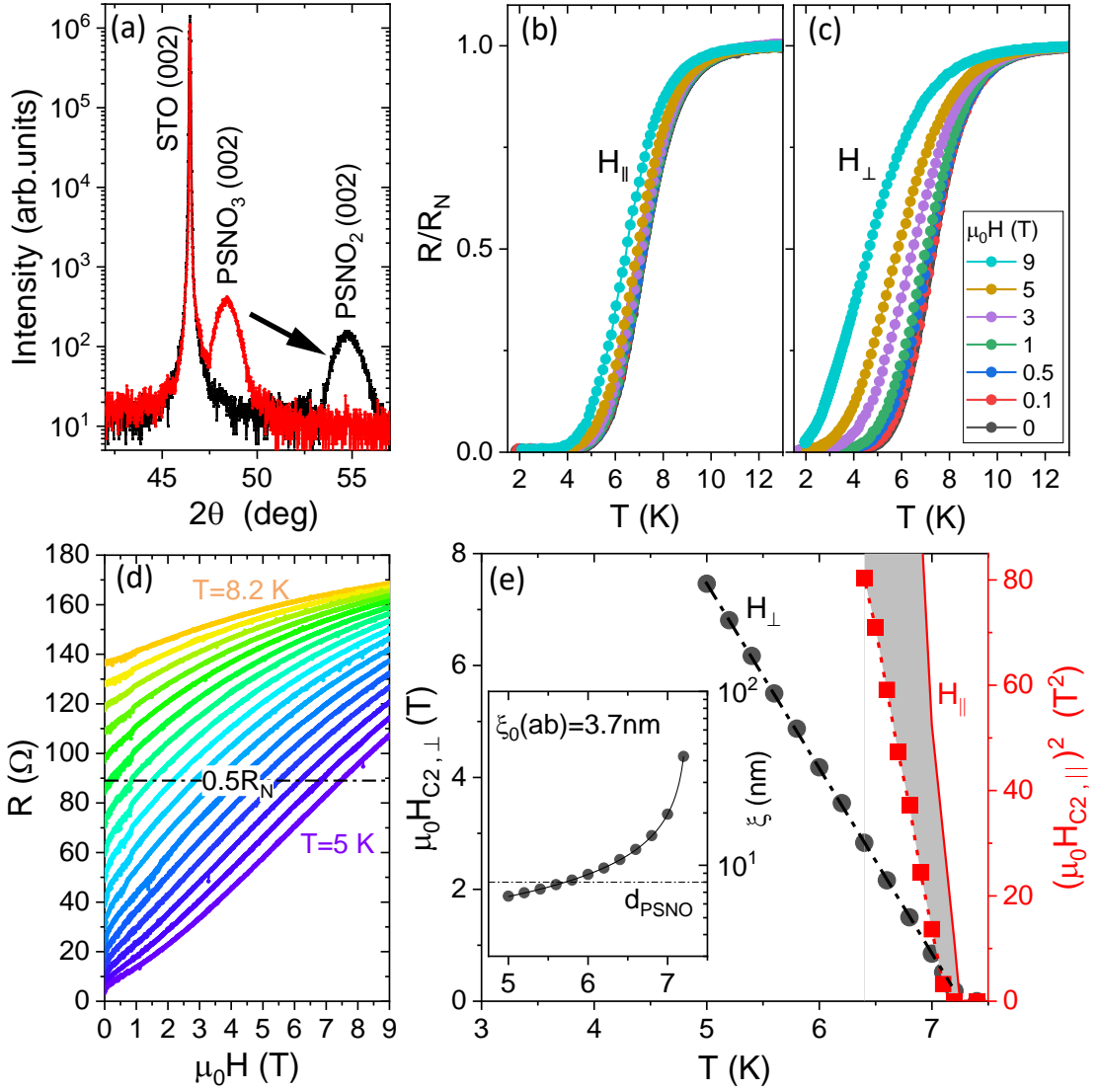


**Figure 1** (a) XRD  $\theta$ - $2\theta$  scan of a PSNO film as-grown (red) and after the  $\text{CaH}_2$  reduction process (black). (b) Normalized resistance vs temperature  $T$  of an IL-PSNO film, measured with  $I = 10 \mu\text{A}$  in magnetic fields  $H$  (see legend) applied parallel and (c) perpendicular to the  $ab$  plane. (d) Resistance vs.  $H$  applied along the  $c$  axis, for  $5 \text{ K} < T < 8.2 \text{ K}$ . The horizontal line indicates the resistance criterion used to determine the upper critical field  $H_{c2,\perp}$ . (e)  $H_{c2,\perp}$  (left axis) and  $(H_{c2,\parallel})^2$  (right axis) vs  $T$ , respectively measured with the field applied perpendicular and parallel to the  $ab$  plane. Lines are a guide to the eye. The grey shadow highlights the difference between  $(H_{c2,\parallel})^2$  and the expectation from Eq. 2 (red solid line). Inset: coherence length in the  $ab$  plane  $\xi(ab)$  vs.  $T$ . The horizontal dashed line indicates the film thickness  $d_{\text{PSNO}}$ , for reference.

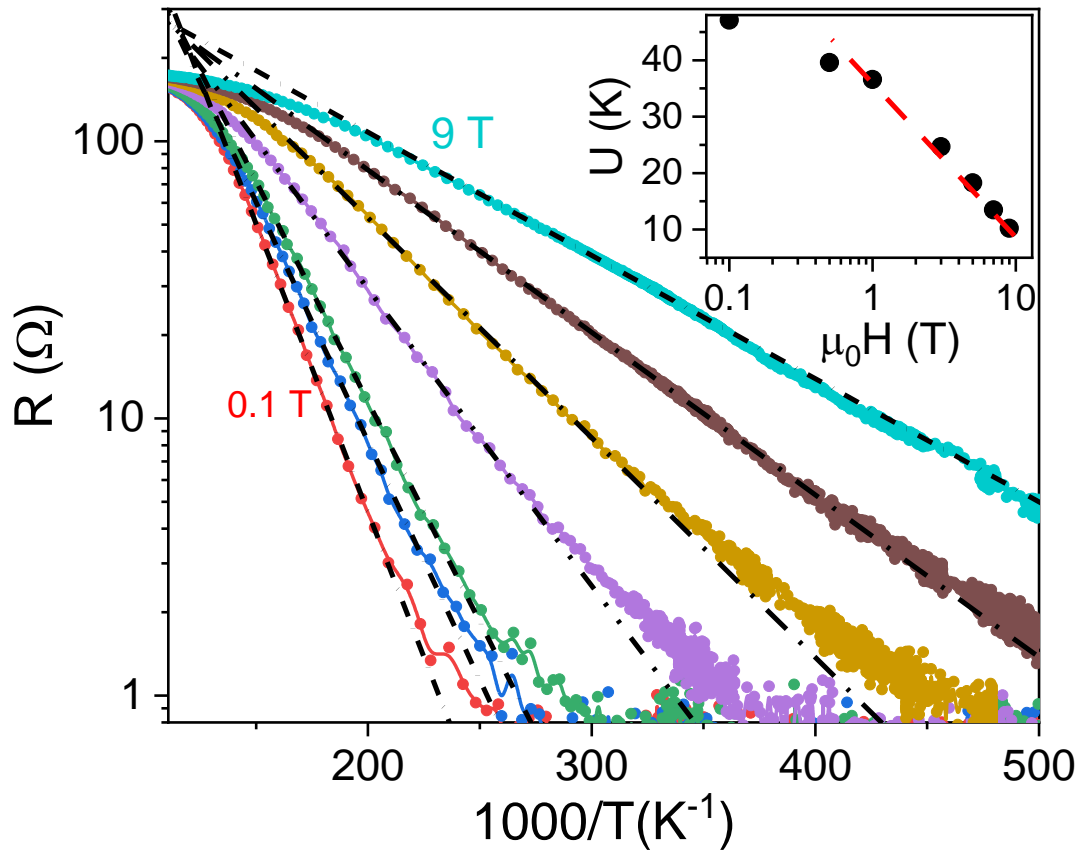


**Figure 2.** Resistance vs  $1000/T$  for magnetic fields between 0.1 and 9 T applied parallel to the  $c$ -axis. Black dashed lines are linear fits. Inset: Magnetic field dependence of the activation  $U$ . The red line is a fit to a logarithmic decay for  $\mu_0 H > 0.5$  T.



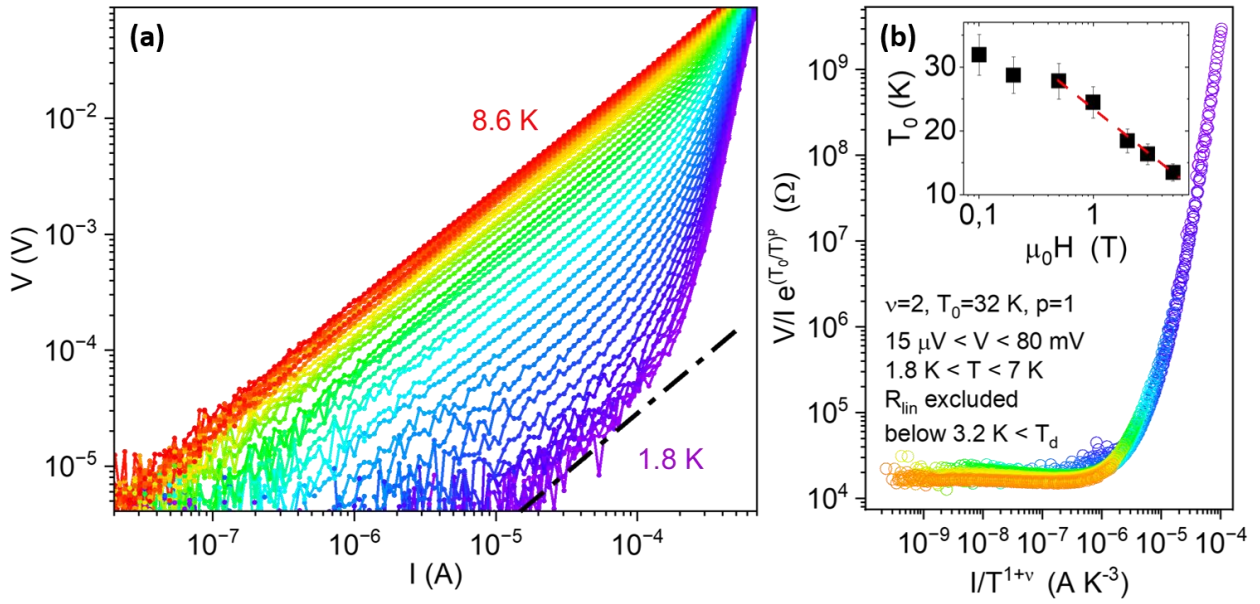


**Figure 3** (a) Voltage vs current isotherms under 0.1T applied parallel to the c-axis, for temperatures between 1.8 and 8.6 K in  $\sim 0.2$  K steps. (b) Scaling of the isotherms following a pure 2D vortex glass model. The scaling parameters are shown in the legend. The inset shows the dependence of  $T_0$  on applied field. The red line is a fit to a logarithmic decay for  $\mu_0 H > 0.5$  T.

## Suppelemental Material for

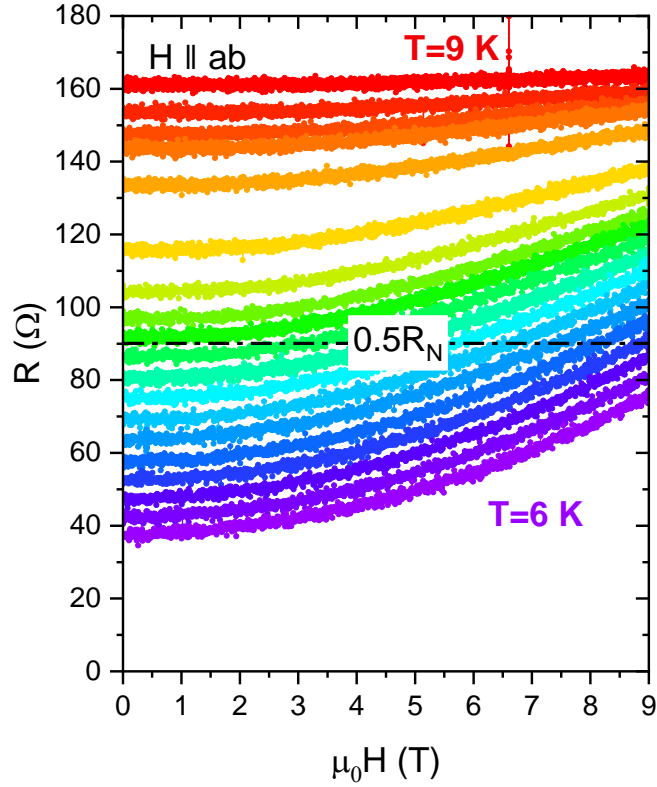
# Purely two-dimensional vortex matter in infinite-layer nickelates

D. Sanchez-Manzano<sup>1</sup>, V. Humbert<sup>1</sup>, A. Gutiérrez-Llorente<sup>2,1</sup>, D. Zhang<sup>1</sup>, J. Santamaría<sup>3</sup>, M. Bibes<sup>1</sup>, L. Iglesias<sup>1,\*</sup>, Javier E. Villegas<sup>1,&</sup>

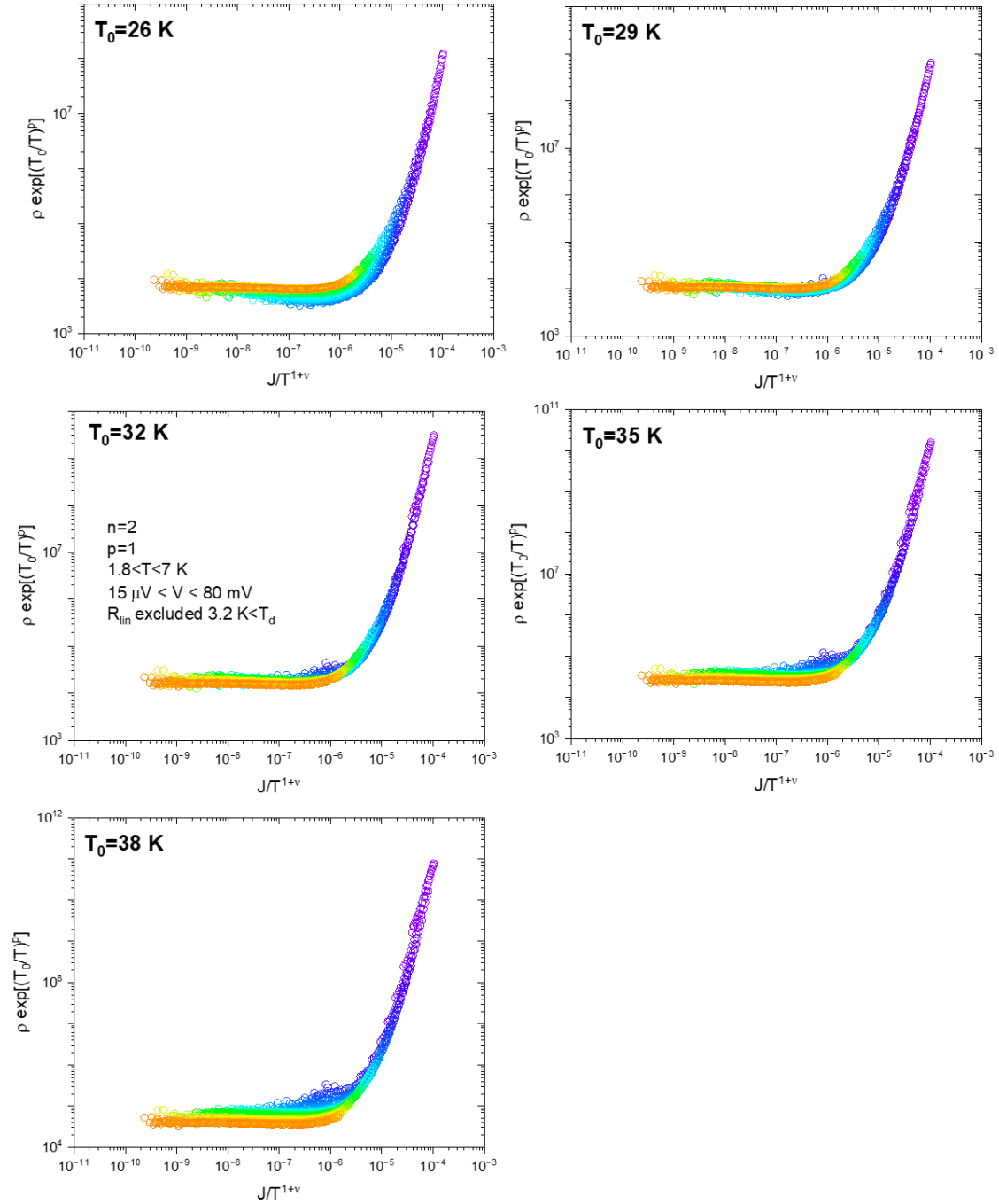
<sup>1</sup>Laboratoire Albert Fert, CNRS, Thales, Université Paris-Saclay, 91767 Palaiseau, France

<sup>2</sup>Escuela Superior de Ciencias Experimentales y Tecnología, Universidad Rey Juan Carlos, 28933 Madrid, Spain

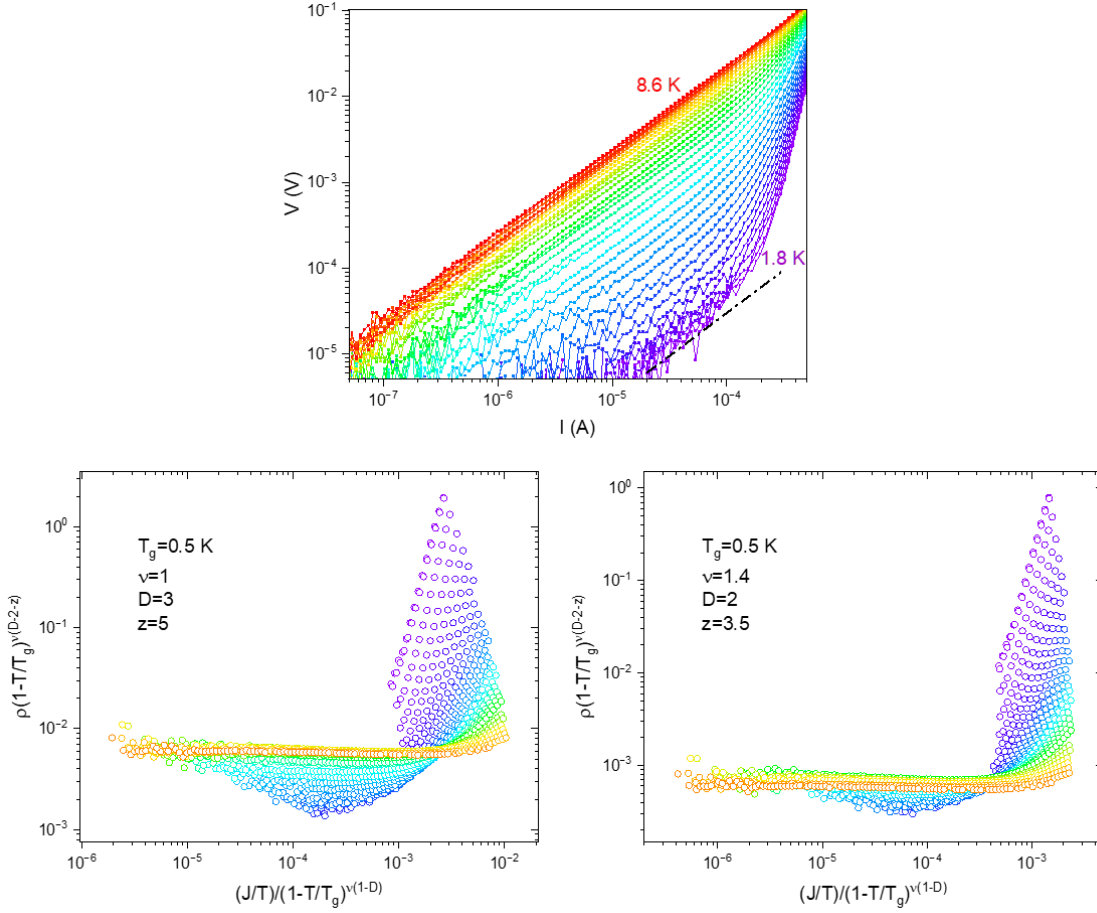
<sup>3</sup>GFMC, Dpto. de Física de Materiales, Facultad de Ciencias Físicas, Universidad Complutense de Madrid, 28040 Madrid, Spain



**Supplementary Figure 1:** Resistance vs.  $H$  applied along the  $ab$  axis, for  $6\text{ K} < T < 9\text{ K}$ . The horizontal line indicates the resistance criterion used to determine the upper critical field  $H_{c2}$ .



**Supplementary Figure 2:** Scaling of the  $V(I)$  dataset shown in Fig. 3 (a), using different values of the scaling parameter  $T_0$ . When  $T_0$  is around 10% off the optimum  $T_0 = 32 \text{ K}$ , a sensible degradation of the data collapse is observed. The degradation becomes much stronger when  $T_0$  is 20% off. This gives a sense of how critical the scaling parameter is, and how precisely it can be determined.



**Supplementary Figure 3:** The vortex-glass transition in 3D or quasi-2D systems occurs at finite  $T_g$ , below which  $V(I)$  become concave downward, yielding a truly superconducting state with  $\lim_{I \rightarrow 0} V/I = 0$ . However, as shown in the example above for  $\mu_0 H = 0.1$  T, all  $V(I)$  show upward curvature in the entire experimental window. The behavior is similar for all sets of  $V(I)$  measured under fields  $0.1 \text{ T} < \mu_0 H < 5 \text{ T}$ . The question that arises is whether  $T_g$  could be finite but lie below the temperature floor of our experiments  $\sim 1.8$  K. The pure 2D scaling discussed in the main text rules out that possibility. To further strengthen this conclusion, we attempted collapsing the  $V(I)$  sets via the scaling ansatz from the vortex-glass theory for 3D or quasi-2D systems [1–3] :

$$(S1) \quad (V/I) |1 - T/T_g|^{v(D-2-z)} = g_{\pm} \left( (I/T) |1 - T/T_g|^{v(1-D)} \right)$$

Where  $g_{\pm}$  is a (field-dependent) universal function for all  $T$  above (+) and below (-)  $T_g$ ,  $D = 3$  for three-dimensional and  $D = 2$  for quasi-two-dimensional systems, and  $z$  and  $\nu$  are respectively the static and dynamic critical exponents which, according to the theory [1], should take values in the ranges  $4 < z < 6$  and  $1 < \nu < 2$ . We tried to collapse the experimental data using Eq. S1 and varying all the parameters  $D, z, \nu$  and  $T_g$  within the physical ranges, with absolutely no success (see examples above), not even being able to collapse the thermally activated flux flow branch  $g_+$  for any  $T_g < 1.8$ .